Quantum Tunnelling Driven H_2 Formation on Graphene

Erxun Han,[†,‡,△] Wei Fang,[¶,§,‖,△] Michail Stamatakis,[⊥] Jeremy O. Richardson,[‖] and Ji Chen[*,†,‡,#,@]

†*School of Physics, Peking University, Beijing 100871, China*

‡*Interdisciplinary Institute of Light-Element Quantum Materials and Research Center for Light-Element Advanced Materials, Peking University, Beijing 100871, People's Republic of China*

¶*State Key Laboratory of Molecular Reaction Dynamics and Center for Theoretical Computational Chemistry, Dalian Institute of Chemical Physics, Chinese Academy of Sciences, Dalian 116023, P. R. China.*

§*Department of Chemistry, Fudan University, Shanghai 200438, China*

‖*Laboratory of Physical Chemistry, ETH Zurich, CH-8093 Zurich, Switzerland*

⊥*Thomas Young Center and Department of Chemical Engineering, University College London, Torrington Place, London WC1E 7JE, United Kingdom*

#*Frontiers Science Center for Nano-Optoelectronics, Peking University, Beijing 100871, People's Republic of China*

@*Collaborative Innovation Center of Quantum Matter, Beijing 100871, People's Republic of China*

△*Contributed equally to this work*

E-mail: ji.chen@pku.edu.cn

Abstract

It is commonly believed that it is unfavourable for adsorbed H atoms on carbonaceous surfaces to form H_2 without the help of incident H atoms. Using ring-polymer instanton theory to describe multidimensional tunnelling effects, combined with *ab initio* electronic structure calculations, we find that these quantum-mechanical simulations reveal a qualitatively different picture. Recombination of adsorbed H atoms, which was believed to be irrelevant at low temperature due to high barriers, is enabled by deep tunnelling, with reaction rates enhanced by tens of orders of magnitude. Furthermore, we identify a new path for H recombination that proceeds via multidimensional tunnelling, but would have been predicted to be unfeasible by a simple one-dimensional description of the reaction. The results suggest that hydrogen molecule formation at low temperatures are rather fast processes that should not be ignored in experimental settings and natural environments with graphene, graphite and other planar carbon segments.

Quantum tunnelling, the classically-forbidden transmission of particles through high-energy barriers, plays an important role in many physical, chemical and biological processes.[1–4] Quantum tunnelling can induce phase transitions,[5] transfer protons[6–10], and change the dynamics of water on surfaces,[11] to name just a few. Despite its importance, the vast majority of previous studies neglect quantum tunnelling effects, in part due to the challenges involved in accurate computational modelling of multidimensional tunnelling. While such an approximation is valid in many circumstances, particularly for processes at high temperatures, it can be problematic at low temperatures and especially for processes involving hydrogen (see *e.g.* refs.[5,12]).

Among all the interesting processes involving hydrogen, adsorption and H_2 formation on graphene is of great importance, and has garnered enormous interest and enthusiasm in many fields. For instance, graphene/graphite based materials can be used as a promising atomic hydrogen storage "warehouse".[13] The abundance of H_2 in outer space is heavily linked to H_2 formation on carbonaceous surfaces of interstellar dust grains.[14] More recently, H_2 formation on graphene has also been attributed to enabling the unexpected permeability of H_2 through graphene.[15] Therefore, the interaction of hydrogen with graphene/graphite, polycyclic aromatic hydrocarbons (PAHs), and other carbonaceous surfaces has been the focus of a large number of studies, see e.g. refs[16–22] for several notable examples.

Hydrogen atoms can adsorb on graphene/graphite surface in a stable chemisorbed state and a less stable physisorbed state.[20] Previous studies have established a picture of H_2 formation on graphene/graphite,[14] consisting of two mechanisms: (i) collision of an incident H atom with a chemisorbed H atom on the surface, known as the Eley–Rideal (ER) mechanism; (ii) combination of two physisorbed H atoms, which is a Langmuir–Hinshelwood (LH) type mechanism. It has been long believed that the LH type mechanism for two chemisorbed H atoms is almost impossible in the cold (and even the moderately warm) regions of interstellar medium, where the temperature ranges from *ca.* 10–200 K. However, this established picture is mostly based on classical-mechanical arguments that the potential-energy barriers

for the diffusion and recombination of chemisorbed H atoms are too high to be relevant.[23] Meanwhile, experimental measurements have indicated that the rate of hydrogen molecule formation is much larger than predictions from simple models based on classical theory.[24] It remains to be unveiled whether quantum mechanics will rewrite our understanding of the mechanism of H_2 formation on graphene.

The past decade saw a blossom of advances in methodology for treating nuclear quantum effects (NQEs), in particular the development of path integral based methods.[25,26] This contributed to a significant leap in the predictive power of computational modelling and vastly enriched our understanding of NQEs in a wide range of systems.[27] Using these methods the adsorption of single H atom on PAH and graphene, has been investigated and exciting results were reported on how NQEs significantly accelerate the hydrogen adsorption process at low temperatures.[20,21,28] These encouraging findings suggest that there is still a lot to be learned regarding the quantum nature of H_2 formation on graphene/graphite. However, a full quantum mechanical treatment of hydrogen molecule formation on surface is a much more challenging task than the study of the adsorption of a single hydrogen atom, demanding a multidimensional tunnelling treatment in conjunction with an on-the-fly *ab initio* treatment of many surface atoms. On one hand, although path integrals molecular dynamics based methods are well implemented within *ab initio* framework, they remain computationally very expensive at low temperatures. On the other hand, instanton theory for treating quantum tunnelling is mostly applied based on classical potential energy surfaces, which may neglect important effects of environment.[29]

In this work, we report a thorough quantum-mechanical investigation of H_2 formation on graphene, with the aim of understanding NQEs in H_2 formation on graphene and other carbonaceous surfaces. We employ ring-polymer instanton theory[29–32], a state-of-the-art method for modelling multidimensional quantum tunnelling in chemical reactions that can capture the mechanistic difference between quantum and classical reaction pathways, in combination with *ab initio* electronic structure calculations performed on-the-fly. Overall,

we see that the H_2 formation rates can be increased by tens of orders of magnitude due to quantum tunnelling, allowing the classically forbidden LH mechanism at chemisorption sites. It is of particular interest that multidimensional tunnelling effects, such as "quantum corner-cutting", play a crucial role. Finally, we employ kinetic Monte Carlo (KMC) simulations to establish a complete picture of the H_2 formation processes on graphene, taking into account all competing processes. The new H_2 formation process identified improves significantly the comparison of theory to available experimental data, hence we propose possible experimental settings to further validate our model.

Our density-functional theory calculations were carried out using the Vienna *ab initio* simulation package (VASP).[33,34] The Perdew-Burke-Ernzerhof (PBE)[35] exchange-correlation functional was used along with the D3 correction[36] to account for van der Waals interactions. The climbing image nudged elastic band (CI-NEB) method[37] was used to obtain the potential energy barriers and minimum energy pathways (MEP) in mass-weighted coordinates. Quantum tunnelling rates and pathways were computed with ring-polymer instanton rate theory[29,30] and extrapolated to the infinite-bead limit.[38] The multidimensional instantons were obtained via first-order saddle-point optimisations at different temperatures with the total force converged to below 0.02 eV·Å^{-1}. The potential energy surface was calculated on-the-fly with DFT, performed using a python wrapper. 64 beads were used to represent the instantons, which was found to give converged results. We used the GT-KMC framework as implemented in the software Zacros[39–41] to simulate hydrogen formation. More computational details and convergence tests are presented in supplementary information (SI).

An overview of the system and the processes that can occur on the surface is presented in Fig. 1a. As a single H atom approaches a graphene surface (or similarly on graphite), it first forms a physisorbed state under the effect of van der Waals (vdW) interactions, with an energy well of 40 meV at the height of ∼3.0 Å above the surface.[20] Then as the H atom moves closer to the surface, at the height of ∼1.5 Å, it finds itself trapped in a chemisorbed state, which is ∼0.75 eV more stable than the physisorbed state (Fig. 1c). The C-H bond length is

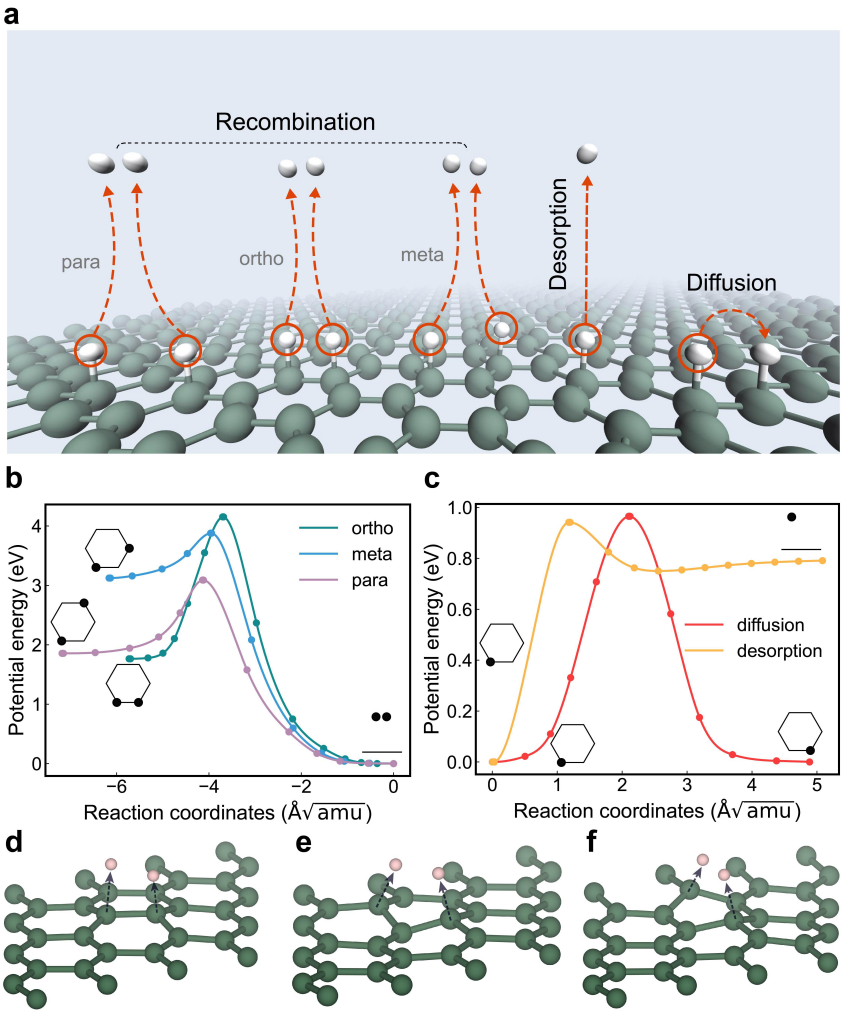

Figure 1: **Classical pathways of key processes of hydrogen formation on graphene.** (a) A schematic showing the Langmuir-Hinshelwood recombination, diffusion, and desorption processes on graphene. Hydrogen and carbon atoms are coloured white and grey-green, respectively. Potential energy profile along the (mass-weighted) intrinsic reaction coordinate[42] for (b) H recombination and (c) H diffusion and desorption/adsorption on graphene. The insets illustrate the H positions at the corresponding points on the potential energy profiles. (d)-(f) Geometries of the transition states of H recombination processes starting from ortho, meta and para adsorption sites.

1.13 Å, with the carbon atom puckering out of the graphene plane by 0.35 Å, featuring a sp^3 hybridisation.[43] A relatively low barrier of 0.2 eV exists for the transition from physisorption to chemisorption, although it was believed to be large enough that this transition is very difficult below room temperature.[44] However, it has been shown that there are many factors, including nuclear quantum effects, that can dramatically increase the likelihood of H atoms chemisorbing on graphene.[18,20,21] For chemically adsorbed H dimers on graphene, according to the adsorption sites of two H atoms on a hexagon, there are three possible configurations, labelled as ortho, meta, and para as shown in Fig. 1a. The most stable adsorption site is the ortho site, which has an adsorption energy of -2.83 eV (defined as $E_{\rm ad}^{(n)} = E_{\rm tot}^{(n)} - n \times E_{\rm H} - E_{\rm gra}$, where $E_{\rm tot}^{(n)}$ is the total energy of the system with n adsorbed H atoms, $E_{\rm H}$ is the energy of a free H atom, and $E_{\rm gra}$ is the energy of the relaxed graphene surface). The para site is slightly less stable (by 0.09 eV), while the meta site is the least stable (1.36 eV less stable than the ortho site). The computed formation energy of H_2 is -4.53 eV and thus, as shown in Fig. 1b, recombination into a H_2 molecule is an exoergic process in each case.

We first reexamine the classical picture of H_2 formation from chemisorption sites. All three H dimers can in principle recombine to form H_2 molecules, however, due to the existence of high barriers, it has been long believed that such a process is almost impossible at low temperatures.[18] We identified the minimum energy pathway (MEP) for the three H dimer recombination processes, using the climbing image nudged elastic band (CI-NEB) method. The potential energy profiles along the MEP are shown in Fig. 1b, and the geometries of the classical transition states are presented in Fig. 1d-f. The barriers computed in this work agree well with previous studies.[18,45] Among all the H_2 formation processes, the one starting from the meta configuration has the lowest energy barrier (0.756 eV). However, since the meta site is energetically less stable than the other sites, at thermal equilibrium, one might expect to find only a tiny fraction of H dimers at the meta configuration, at least in the limit where H atoms on the surface are sparse, which would make the effect of the meta pathway negligible. However, if the meta dimer is stabilised, *e.g.* via the formation of stable

H atom trimers that contain the meta configuration, then the meta pathway may become an important contributor to the overall process. Classical mechanics also predicts that the ortho path is unfavourable, as it has the largest potential energy barrier of 2.389 eV. Therefore, one can conclude that classically, H_2 recombination mostly likely happens via the para path, with an energy barrier of 1.234 eV. The classical reaction rate, estimated using Eyring transition-state theory (TST),[46] is $\sim 10^{-4}$ s^{-1} for H recombination from the para site at room temperature and rapidly decreases to $\sim 10^{-13}$ s^{-1} at 200 K (Fig. 2a). This means that classically, recombination processes are unlikely to play a significant role in low-temperature environments.

To shed light on the complete process of H_2 formation, we also computed atomic hydrogen diffusion and desorption MEPs (Fig. 1c). The potential energy barriers of the two processes are almost identical (0.966 eV for diffusion and 0.942 eV for desorption), meaning that classically, desorption and diffusion events occur with similar frequencies. This suggests that long-range diffusion of chemisorbed H atoms on graphene is almost impossible classically,[47] which would imply that H clusters on graphene cannot be formed via surface diffusion. Nevertheless, it has been shown that H clusters can form directly on graphene or graphite due to preferential sticking into specific adsorbate structures.[18] The desorption process also has a lower barrier than the H_2 formation processes from the stable para and ortho sites, suggesting that recombination is much less likely than for a single H atom to desorb from the surface. These findings fully agree with the previous studies based on classical mechanics indicating that the LH mechanism is gravely unfavourable for chemisorbed H atoms.[23]

Due to the light mass of hydrogen, the adsorption, diffusion, and recombination processes are quantum mechanical in nature. For this reason we must account for nuclear quantum effects, particularly tunnelling, in our simulations especially at low temperatures. As a first step towards understanding the importance of tunnelling, we computed the crossover temperature,[48,49] given by $T_c \approx \frac{\hbar\omega^{\ddagger}}{2\pi k_B}$, where $\omega^{\ddagger}$ is the magnitude of the imaginary frequency at the transition state. T_c is the temperature at which the instanton (which represents an

optimal tunnelling pathway) starts to delocalise across the barrier and thus it provides an estimate of the temperature below which tunnelling should be considered in a given process. The three H recombination pathways all have high values of T_c above 400 K (see SI.II), suggesting that H_2 formation will exhibit strong tunnelling effects even at room temperature. The temperatures in interstellar environments and many experimental settings are well below the crossover temperature, such that H_2 formation is driven by very deep tunnelling, which would fundamentally invalidate the classical picture.

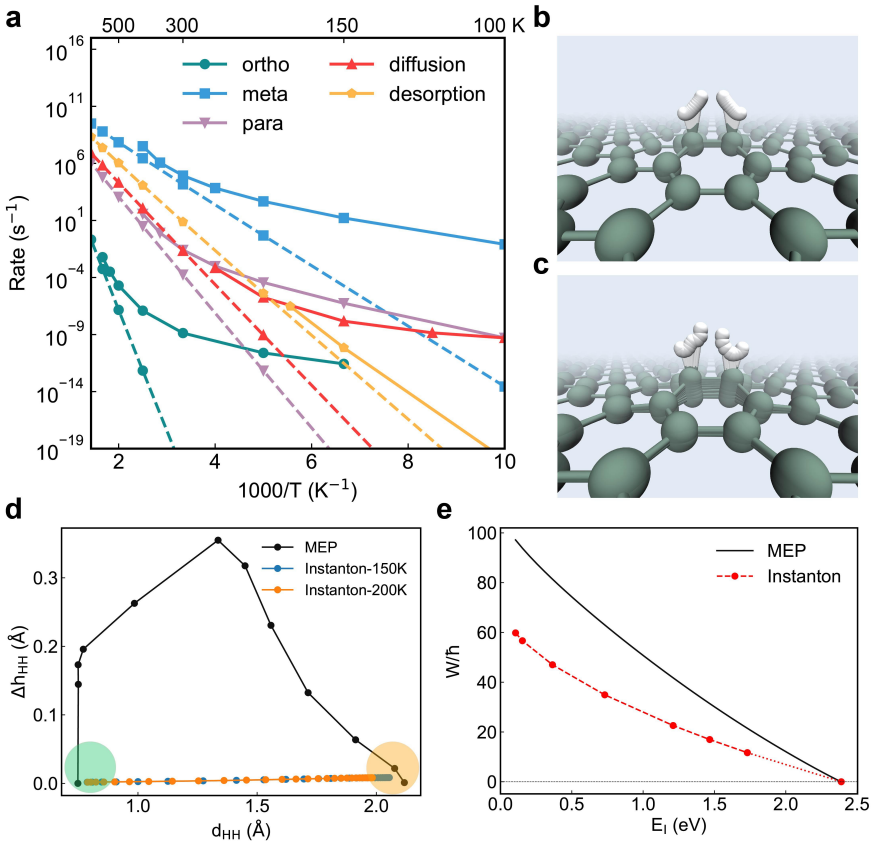

Figure 2: **Quantum and classical reaction rates and pathways.** (a) On-the-fly instanton rates (solid lines) and Eyring transition-state theory (TST) rates (dashed lines) for H recombination, diffusion, and desorption. Geometry of (b) the instanton trajectory and (c) the minimum energy pathway (MEP) for H recombination from the ortho site at 150 K. (d) Comparison of the MEP and the instanton pathways within a 2D representation. d_{HH} represents the distance between the two H atoms and Δh_{HH} is the height difference of the atoms with respect to the graphene plane. The green region indicates the final state and the orange region indicates the initial state. (e) Comparison of the abbreviated action (W) (see SI Eq. 2) calculated along the minimum energy pathway (MEP) and along instanton trajectories. E_I represents the instanton energy or the energy along the reaction coordinate.

Using ring-polymer instanton theory with the potential energy surface generated on-the-fly with DFT, we thoroughly investigated the role of tunnelling in this system over a wide range of temperatures to uncover the quantum picture. The technical details necessary to overcome computational challenges in these calculations and the validation tests are discussed in SI.I. For the diffusion and desorption processes, quantum effects flipped the table. Unlike in the classical picture, the instanton rate for the diffusion process greatly exceeds that of the desorption process at temperatures below 200 K (see Fig. 2a). In fact, the desorption process shows only minor tunnelling contributions and the instanton rate[50] displays a near Arrhenius behaviour over all temperatures considered, while the diffusion rate is strongly non-Arrhenius and the rate becomes weakly temperature dependent at ∼100 K, which is a signature of deep tunnelling. Therefore, in the quantum picture, tunnelling can enable long-range diffusion for a H atom, promoting its mobility even at low temperatures, without being desorbed from the surface. Quantum diffusion can therefore also facilitate the formation of H clusters on graphene. The inability of tunnelling to accelerate the desorption process is because it is endothermic by 0.75 eV. Even though tunnelling can accelerate the barrier crossing, it cannot break energy conservation, meaning that the reactant must still be thermally activated by at least 0.75 eV before it can desorb from the surface.

Tunnelling also dominates the H recombination processes. Instanton rates show strong non-Arrhenius behaviour for all three recombination pathways (Fig. 2a). For the ortho pathway, even at room temperature, tunnelling plays a significant role in increasing the rate by ∼10 orders of magnitude. The extraordinarily high tunnelling factor results from a combination of features in this pathway, such as short path length, high barrier, high T_c, and strong corner-cutting effects, which all act to enhance the tunnelling factor. At 150 K, the tunnelling factor for this pathway increases by 44 orders of magnitude. Strong tunnelling is also seen in the para pathway at low temperature, i.e. at 100 K where tunnelling increases the rate by almost 30 orders of magnitude. However, compared to the ortho pathway, the increase is less dramatic mainly due to the longer tunnelling distance. As a result, the rate difference

between the two pathways (ortho and para) is greatly reduced in the quantum scenario. This means that the para pathway may no longer be the only favourable recombination pathway and that the ortho pathway could also play an important role in the quantum scenario, especially bearing in mind that it will be more populated at thermal equilibrium. There is also a significant tunnelling effect for the meta pathway, albeit to a lesser extent than the other two pathways.

Multidimensional tunnelling effects, namely corner-cutting[51,52] where the quantum tunnelling pathway deviates from the classical MEP, also play a crucial role in the H recombination processes. The classical reaction pathway for the ortho site (Fig. 2c) involves a stepwise mechanism where one H atom first breaks the chemical bond to the graphene surface, then recombines with the other H atom to form H_2, which leaves the surface. This mechanism features an asymmetric transition state, where one H is further away from the surface than the other H atom. Yet the mechanism qualitatively changes in the quantum scenario, featuring a symmetric tunnelling pathway where the two H atoms tunnel in a concerted fashion, simultaneously approaching each other and leaving the graphene surface (Fig. 2b). To clearly present the mechanistic change, we show a projection of the pathways onto two generalised coordinates in Fig. 2d. It can be seen that the height difference between the two H atoms varies along the classical pathway but the quantum pathway remains symmetric (within the level of numerical convergence). The qualitative difference between the classical and quantum pathways would invalidate all the MEP based tunnelling correction methods, which are commonly used to predict tunnelling rates in chemical reactions.[53,54] In fact, the abbreviated action, which characterises the difficulty of transmission through a tunnelling pathway, is significantly lower on the optimal tunnelling pathways (instantons) than on the MEP (Fig. 2e). This indicates that MEP based methods could underestimate the tunnelling rate by $\sim$10 orders of magnitude for the ortho pathway in the deep tunnelling case (see SI.III).

The ortho pathway is not the only pathway impacted by strong quantum corner-cutting

effects. We show in SI.II that the instanton path deviates from the MEP for all three H recombination pathways. For the para pathway, despite no qualitative mechanistic difference between the classical and the quantum scenario, using the MEP still severely underestimates tunnelling compared to the instanton theory. By carefully comparing the MEP and the instantons, we find that the quantum corner-cutting effects in the para pathways mainly come from the fact that the optimal tunnelling pathway makes a compromise between minimising the potential energy along the path and trying to avoid tunnelling in the heavier C atoms, which is unfavourable. Indeed, we can see that even for the deep tunnelling instantons at the lowest temperature studied, only limited carbon tunnelling is observed (see Fig. 2b). Overall, the strong quantum corner-cutting effects are widely observed in H atom processes on graphene with quantum tunnelling considered, which reveal the qualitative difference between the quantum and classical reaction pathways in multidimensional space.

Moreover, the dominance of nuclear quantum tunnelling predicted in our study is expected to lead to strong kinetic isotope effects (KIEs).[55,56] Due to the fact that the richness of deuterium (D) is low (less than 1%), the most likely process would be the formation of HD, while D_2 formation would be very rare. Therefore, we analyse the formation of HD molecules via a Langmuir-Hinshelwood (LH) type mechanism from chemisorbed hydrogen and deuterium using multidimensional instanton theory. The instanton trajectories for HD formation becomes "asymmetric" (see Fig. S6), as the tunnelling distance of H and D atoms differ due to their mass differences (D is heavier and less likely to tunnel). Despite this, the HD tunnelling pathway resembles the H_2 tunnelling pathway rather than the MEP, even for the ortho pathway, suggesting that the corner-cutting effects also play a significant role in HD formation. At 150K the rates of HD formation via ortho and para pathways decrease by 3 orders of magnitude compared to the formation rates of H_2 (Table I). The rates of the ortho and para path differ by 3 orders of magnitude for HD formation, suggesting that the ortho path is less important compared to H_2 formation. We also expect that recombination rates are further decreased when we consider two deuterium (or tritium) atoms forming D_2 (or

T_2). Based on the Bell-Limbach tunnelling model,[57] the formation rate of D_2 would be more than 6 orders of magnitude lower than the formation rates of H_2. These results are in line with the current understanding that in outer space the isotopic fractionation of deuterium goes through a different path involving other larger molecules.[58] The strong isotope effects also suggest that delicate isotopic control of H_2 formation may be achievable.

Table 1: Multidimensional instanton rates for H_2 and HD formation processes at 100 K (150 K for formation on ortho site).

Process	Multidimensional instanton rates (s^{-1})	
	H_2	HD
Ortho	3.25×10^{-12} (150 K)	8.97×10^{-16} (150 K)
Meta	1.03×10^{-1}	1.54×10^{-3}
Para	6.82×10^{-10}	8.28×10^{-13}

The previous sections discussed the H_2 formation rates from H dimers, which corresponds to the situation in the sparse-coverage limit. However, H-rich regions may also exist, and since H_2 formation on graphene involves several sub-processes, to better understand the overall mechanism when the H atoms are not sparse, we further employ Graph-Theoretical Kinetic Monte Carlo (GT-KMC) simulations[39–41] to calculate the occurrence frequencies for the different sub-processes. The GT-KMC simulations are initialised with H atoms randomly adsorbed on the lattice and a queue containing all the possible processes for the given configurations. The queue then stores the waiting times corresponding to each elementary event, which is used to propagate the state of the KMC simulation. Notably, while the GT-KMC occurrence frequencies are closely related to the rates of the individual processes, they are certainly different, as GT-KMC takes into account the cooperation and competition between the different processes as well as the effect of lateral interactions between H adatoms on the reaction rates and offers insights from a different perspective.

We focus on the low-temperature regime at 100 K. For the ortho path, the instanton rate at 150 K is used in our KMC model for the quantum scenario and, as one can see from Fig. 2, the rate has become weakly temperature dependent by 150 K, a signature of deep

tunnelling. One can see from Fig. 3 that the classical and quantum (instanton) scenarios differ drastically. Classically, H atoms are effectively frozen on the graphene surface as diffusion and recombination processes have exceedingly low occurrence frequencies. Quantum tunnelling significantly enhances the event occurrence frequency of these processes by ∼30 orders of magnitude. The GT-KMC results also show that at such a low temperature, H atom desorption no longer occurs, even after accounting for quantum tunnelling. These findings are consistent with the classical and quantum rates discussed in the previous sections. More importantly, the GT-KMC results confirm the qualitative difference in the role of the ortho pathway between the classical and quantum scenarios. Classically, the ortho pathway is unfavourable due to the high potential energy barrier. Multidimensional tunnelling effects dramatically boost the rate of the ortho process and the GT-KMC results show that this pathway becomes almost as important as the other two pathways in the quantum scenario.

To visualise the difference, we show snapshots from the GT-KMC simulations with the classical and quantum rates at 100 K in Fig. 3b-c (see the SI for details). In accordance with the discussion on the individual rates, KMC also predicts that, in the classical scenario, H atoms remain adsorbed over a long period of more than 1.5×10^{36} s (i.e. longer than the age of the universe). For the few H atoms that do leave the surface, the desorption process dominates, whereas the H_2 formation processes are rare. However, in the quantum scenario during a significantly shorter period (Fig. 3c) of 2.0×10^{9} s (∼60 years, a relatively short period of time in interstellar space), we observe not only diffusion, but also a large amount of H_2 formation processes (green dots). At the end of the simulation all H atoms have recombined.

In addition to graphene, other carbonaceous materials exist in nature in different forms, hence naturally they can also serve as substrates for H_2 formation. In general, carbon materials can exhibit sp^2 hybridisation (e.g. amorphous carbon and graphene) or sp^3 hybridisation (e.g. diamond). For comparison, we calculate the potential energy barriers for H_2 formation on diamond, fullerene (C_{60}) and amorphous monolayer carbon (AMC) surfaces at different

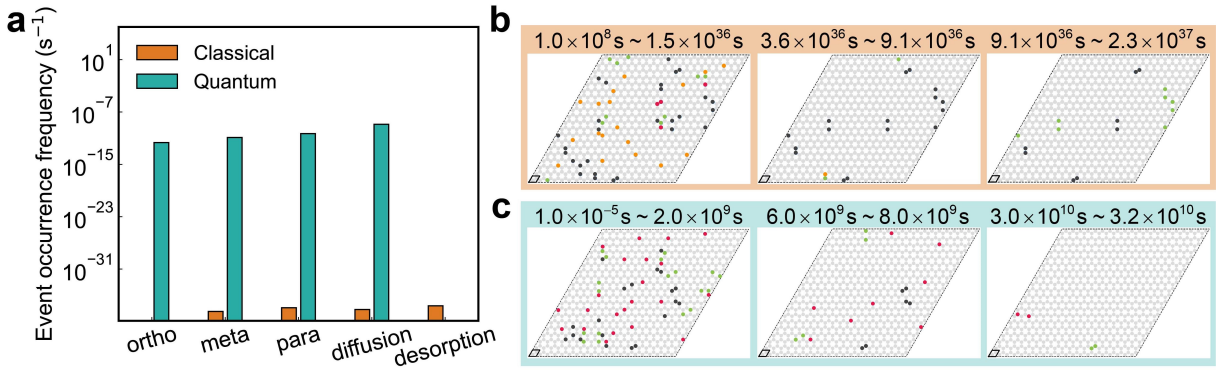

Figure 3: **Event occurrence frequencies of various processes from GT-KMC simulations.** (a) Comparison of the classical and quantum event occurrence frequencies of H diffusion, desorption, and recombination on graphene at 100 K. Representative windows of KMC simulations at 100 K for (b) the classical scenario and (c) the quantum scenario. Note that different timescales are displayed in the two cases. For each window, H atoms that diffuse are coloured red. H atoms that desorb or recombine as H_2 are coloured orange and green, respectively. Immobile H atoms are coloured as black.

adsorption sites using the CI-NEB method (see Fig. 4). The detailed formation configurations are provided in SI.VI. Overall, the energy barriers rise as the energy difference between the final and the initial state increases, qualitatively satisfying the Bell–Evans–Polanyi (BEP) principle[59] which predicts a linear relation between the activation energy and the enthalpy of reaction. On the diamond surfaces, the associative H_2 desorption processes are endothermic by more than 2 eV in each case, and correspondingly the barriers are at least 3 eV, meaning that H_2 formation is unfavourable on this type of surface. We attribute this to the strong chemical binding of the hydrogen to sp^3 carbon surfaces. On the AMC surfaces, all formation processes exhibit large barriers of more than 2.3 eV, which are close to the highest energy values on graphene, suggesting that H_2 formation via classical over-the-barrier processes on AMC is more difficult than on graphene. It is however possible that H_2 formation on AMC could be enabled by quantum tunnelling, similarly to the case of the ortho pathway on graphene. However, diffusion via tunnelling on AMC could be hampered by the fact that different sites on the surface having different binding energies, meaning that some thermal activation will be necessary such that H atom clusters might be difficult to form on AMC at low temperatures. On fullerene (C_{60}) we found two pathways with relatively low barriers,

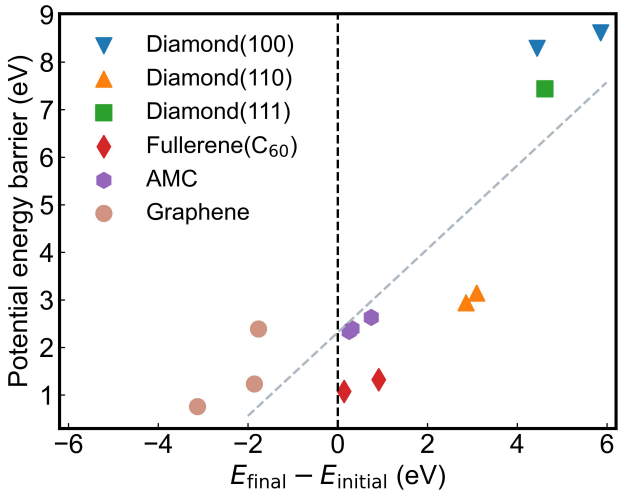

Figure 4: **H_2 formation on carbonaceous surfaces.** The vertical axis plots the potential energy barriers for H_2 formation on several carbonaceous surfaces obtained by CI-NEB calculations. $E_{\text{final}} - E_{\text{initial}}$ is the energy difference between the final and the initial state of the formation process. The vertical dashed line separates the exothermic and the endothermic regimes, and the grey dashed line qualitatively describes the roughly linear correlation between the barrier and the energy difference.

one of which is even lower than the para pathway on graphene and is only slightly endothermic. The potential energy curves of these processes are also shown in SI.VI. The curvature at the barrier top is often a good indicator of the strength of nuclear quantum effects. The pointy the barrier, the higher the crossover temperature, the stronger the tunnelling effects. We see that on C_{60} and AMC, two systems that have similar bonding to graphene, the barriers also have similar curvature to graphene. The larger curvature can be attributed to the early breaking of C-H bonds before approaching the transition state, which shorten the evolving distance of C atoms. Therefore, we can conclude that all the non-amorphous sp^2 carbon materials which we tested (i.e. graphene and fullerene) are favourable substrates for H_2 formation.

To conclude, by extensively studying hydrogen formation processes on graphene, we revealed that the H_2 formation mechanisms fundamentally change between the classical and quantum scenarios at low temperatures. It was widely believed that the LH mechanism for chemisorbed H atoms does not occur due to the low diffusion rates of H atoms adsorbed

on the surface, which are thought to prevent long-range H diffusion. We argue that such a picture is only true in the classical scenario. With quantum mechanics, H diffusion can occur at the temperatures and timescales of the interstellar medium, as quantum tunnelling drastically accelerates the diffusion process but not the desorption process. Classically, it is believed that the recombination of chemisorbed H atoms only occurs via the para site, and that recombination from the ortho site is impossible due to the high barrier. Yet, quantum tunnelling enables the ortho recombination mechanism by enhancing the rate by tens of orders of magnitude, making this mechanism more competitive at low temperatures. The tunnelling pathway for the ortho mechanism qualitatively differs from the classical pathway due to strong multidimensional quantum corner-cutting effects, featuring a concerted recombination mechanism instead of a stepwise one.

Theoretically, it is well known that DFT underestimates the barriers for covalent bond breaking or formation processes due to the self-interaction error. Thus, as a first step towards the quantitatively exact treatment we examine the influence of self-interaction error on our results by testing a hybrid functional, namely the HSE06 functional[60] with D3 dispersion corrections.[36] As discussed in detail in SI.VII, we found that this change does not have any qualitative impact on our conclusions, and quantitatively it brought the rate of the ortho path even closer to the rate of the para path, further strengthening the finding that the ortho path is important in the quantum scenario. In the future, when on-the-fly instanton theory is combined with more accurate electronic structure, quantitative prediction of tunnelling dominant reaction is foreseeable. We also note that our theoretical discussions are within the Born-Oppenheimer approximation and have not included non-adiabatic effects. According to previous studies, the dissociation of C-H bond is accompanied by very large excitation energies.[61] Therefore, we do not expect significant non-adiabatic effects for hydrogen recombination, diffusion and desorption processes at low temperatures without external fields.

This work highlights the pivotal impact quantum-mechanical effects can have for surface

processes involving hydrogen, which casts new light on the understanding of H_2 formation on graphene and other carbonaceous surfaces. Although graphene/graphite and their hydrogenated samples are amongst the most well controlled samples which can be nicely investigated with various types of experimental instruments, such measurements have been very rare due to the difficulty in detecting hydrogen and the misconception of the mechanism and speed of H_2 formation. Here, an important fact revealed is that the quantum rates of H_2 formation are within the detectable regimes of many laboratory experimental techniques such as helium and neutron scattering, surface probing, and optical diffraction. Combined with the possibility of visualising the position and vibration of hydrogen using advanced microscopies, experimental studies of H_2 formation on graphene/graphite are desirable to compare with our theoretical predictions. Last but not the least, H_2 formation on other materials may also feature strong tunnelling effects, and we urge experimental works to take tunnelling effects into account in their data analysis.

Acknowledgement

The authors thank X.-Z. Li and Y.-X. Feng for helpful discussions on this topic. This work was supported by the Strategic Priority Research Program of Chinese Academy of Sciences under Grant No. XDB33000000, and the National Natural Science Foundation of China under Grant No. 11974024. We are grateful for computational resources provided by Peking University, the TianHe-1A supercomputer, Shanghai Supercomputer Center, and Songshan Lake Materials Lab.

Supporting Information Available

The Supporting Information is available free of charge.

- Details of calculations and detailed results of this work; Analysis of the quantum and

classical pathways for hydrogen diffusion, recombination, and desorption; Minimum energy pathway based 1D tunnelling corrections; H/D isotope effects; KMC simulation setup and convergence tests; Geometries for hydrogen molecule formation on carbonaceous surfaces; Tests with a hybrid exchange correlation functional.

References

(1) Pu, J.; Gao, J.; Truhlar, D. G. Multidimensional tunneling, recrossing, and the transmission coefficient for enzymatic reactions. *Chem. Rev.* **2006**, *106*, 3140–3169.

(2) Jónsson, H. Simulation of surface processes. *Proc. Natl. Acd. Sci. U. S. A* **2011**, *108*, 944–949.

(3) Meisner, J.; Kästner, J. Atom Tunneling in Chemistry. *Angew. Chem. Int. Ed.* **2016**, *55*, 5400–5413.

(4) Richardson, J. O.; Perez, C.; Lobsiger, S.; Reid, A. A.; Temelso, B.; Shields, G. C.; Kisiel, Z.; Wales, D. J.; Pate, B. H.; Althorpe, S. C. Concerted hydrogen-bond breaking by quantum tunneling in the water hexamer prism. *Science* **2016**, *351*, 1310–1313.

(5) Fang, W.; Chen, J.; Feng, Y.; Li, X.-Z.; Michaelides, A. The quantum nature of hydrogen. *Int. Rev. Phys. Chem.* **2019**, *38*, 35–61.

(6) Drechsel-Grau, C.; Marx, D. Quantum simulation of collective proton tunneling in hexagonal ice crystals. *Phys. Rev. Lett.* **2014**, *112*, 148302.

(7) Litman, Y.; Richardson, J. O.; Kumagai, T.; Rossi, M. Elucidating the nuclear quantum dynamics of intramolecular double hydrogen transfer in porphycene. *J. Am. Chem. Soc.* **2019**, *141*, 2526–2534.

(8) Lam, Y.-C.; Soudackov, A. V.; Hammes-Schiffer, S. Theory of Electrochemical Proton-Coupled Electron Transfer in Diabatic Vibronic Representation: Application to Proton

Discharge on Metal Electrodes in Alkaline Solution. *J. Phys. Chem. C* **2020**, *124*, 27309–27322.

(9) Sakaushi, K. Quantum Proton Tunneling in Multi-Electron/-Proton Transfer Electrode Processes. *Faraday Discuss.* **2019**, *221*, 428–448.

(10) Sakaushi, K.; Lyalin, A.; Taketsugu, T.; Uosaki, K. Quantum-to-Classical Transition of Proton Transfer in Potential-Induced Dioxygen Reduction. *Phys. Rev. Lett.* **2018**, *121*, 236001.

(11) Fang, W.; Chen, J.; Pedevilla, P.; Li, X.-Z.; Richardson, J. O.; Michaelides, A. Origins of fast diffusion of water dimers on surfaces. *Nat. Commun.* **2020**, *11*, 1689.

(12) Sims, I.; Smith, I. Gas-phase reactions and energy-transfer at very-low temperatures. *Annu. Rev. Phys. Chem.* **1995**, *46*, 109–138.

(13) Elias, D. C.; Nair, R. R.; Mohiuddin, T. M. G.; Morozov, S. V.; Blake, P.; Halsall, M. P.; Ferrari, A. C.; Boukhvalov, D. W.; Katsnelson, M. I.; Geim, A. K.; Novoselov, K. S. Control of graphene's properties by reversible hydrogenation: evidence for graphane. *Science* **2009**, *323*, 610–613.

(14) Vidali, G. H_2 formation on interstellar grains. *Chem. Rev.* **2013**, *113*, 8762–8782.

(15) Sun, P. Z.; Yang, Q.; Kuang, W. J.; Stebunov, Y. V.; Xiong, W. Q.; Yu, J.; Nair, R. R.; Katsnelson, M. I.; Yuan, S. J.; Grigorieva, I. V.; Lozada-Hidalgo, M.; Wang, F. C.; Geim, A. K. Limits on gas impermeability of graphene. *Nature* **2020**, *579*, 229–232.

(16) Morisset, S.; Aguillon, F.; Sizun, M.; Sidis, V. Quantum dynamics of H_2 formation on a graphite surface through the Langmuir Hinshelwood mechanism. *J. Chem. Phys.* **2004**, *121*, 6493–6501.

(17) Hornekær, L.; Sljivancanin, Z.; Xu, W.; Otero, R.; Rauls, E.; Stensgaard, I.; Laegsgaard, E.; Hammer, B.; Besenbacher, F. Metastable structures and recombination path-

ways for atomic hydrogen on the Graphite (0001) surface. *Phys. Rev. Lett.* **2006**, *96*, 156104.

(18) Hornekær, L.; Rauls, E.; Xu, W.; Sljivancanin, Z.; Otero, R.; Stensgaard, I.; Laegsgaard, E.; Hammer, B.; Besenbacher, F. Clustering of chemisorbed H(D) atoms on the graphite (0001) surface due to preferential sticking. *Phys. Rev. Lett.* **2006**, *97*, 186102.

(19) Casolo, S.; Tantardini, G. F.; Martinazzo, R. Insights into H_2 formation in space from ab initio molecular dynamics. *Proc. Natl. Acad. Sci. U. S. A.* **2013**, *110*, 6674–6677.

(20) Davidson, E. R. M.; Klimeš, J.; Alfè, D.; Michaelides, A. Cooperative Interplay of van der Waals Forces and Quantum Nuclear Effects on Adsorption: H at Graphene and at Coronene. *ACS Nano* **2014**, *8*, 9905–9913.

(21) Goumans, T. P. M.; Kästner, J. Hydrogen-Atom Tunneling Could Contribute to H_2 Formation in Space. *Angew. Chem. Int. Ed.* **2010**, *49*, 7350–7352.

(22) Petucci, J.; Semone, S.; LeBlond, C.; Karimi, M.; Vidali, G. Formation of H_2 on graphene using Eley-Rideal and Langmuir-Hinshelwood processes. *J. Chem. Phys.* **2018**, *149*, 014702.

(23) Wakelam, V.; Bron, E.; Cazaux, S.; Dulieu, F.; Gry, C.; Guillard, P.; Habart, E.; Hornekaer, L.; Morisset, S.; Nyman, G.; Pirronello, V.; Price, S. D.; Valdivia, V.; Vidali, G.; Watanabe, N. H_2 formation on interstellar dust grains: The viewpoints of theory, experiments, models and observations. *Mol. Astrophys.* **2017**, *9*, 1–36.

(24) Pirronello, V.; Liu, C.; Shen, L. Y.; Vidali, G. Laboratory synthesis of molecular hydrogen on surfaces of astrophysical interest. *Astrophys. J.* **1997**, *475*, L69–L72.

(25) Markland, T. E.; Ceriotti, M. Nuclear quantum effects enter the mainstream. *Nat. Rev. Chem.* **2018**, *2*, 0109.

(26) Richardson, J. O. Perspective: Ring-polymer instanton theory. *J. Chem. Phys.* **2018**, *148*, 200901.

(27) Ceriotti, M.; Fang, W.; Kusalik, P. G.; McKenzie, R. H.; Michaelides, A.; Morales, M. A.; Markland, T. E. Nuclear Quantum Effects in Water and Aqueous Systems: Experiment, Theory, and Current Challenges. *Chem. Rev.* **2016**, *116*, 7529–7550.

(28) Jiang, H.; Kammler, M.; Ding, F.; Dorenkamp, Y.; Manby, F. R.; Wodtke, A. M.; Miller, T. F.; Kandratsenka, A.; Büenermann, O. Imaging Covalent Bond Formation by H Atom Scattering from Graphene. *Science* **2019**, *364*, 379–382.

(29) Richardson, J. O. Ring-polymer instanton theory. *Int. Rev. Phys. Chem.* **2018**, *37*, 171–216.

(30) Richardson, J. O.; Althorpe, S. C. Ring-polymer molecular dynamics rate-theory in the deep-tunneling regime: Connection with semiclassical instanton theory. *J. Chem. Phys.* **2009**, *131*, 214106.

(31) Andersson, S.; Nyman, G.; Arnaldsson, A.; Manthe, U.; Jónsson, H. Comparison of Quantum Dynamics and Quantum Transition State Theory Estimates of the H + CH_4 Reaction Rate. *J. Phys. Chem. A* **2009**, *113*, 4468–4478.

(32) Kästner, J. Theory and Simulation of Atom Tunneling in Chemical Reactions. *Wiley Interdiscip. Rev. Comput. Mol. Sci.* **2014**, *4*, 158–168.

(33) Kresse, G.; Furthmuller, J. Efficient iterative schemes for ab initio total-energy calculations using a plane-wave basis set. *Phys. Rev. B* **1996**, *54*, 11169–11186.

(34) Kresse, G.; Furthmuller, J. Efficiency of ab-initio total energy calculations for metals and semiconductors using a plane-wave basis set. *Comput. Mater. Sci.* **1996**, *6*, 15–50.

(35) Perdew, J. P.; Burke, K.; Ernzerhof, M. Generalized gradient approximation made simple. *Phys. Rev. Lett.* **1996**, *77*, 3865–3868.

(36) Grimme, S.; Antony, J.; Ehrlich, S.; Krieg, H. A consistent and accurate ab initio parametrization of density functional dispersion correction (DFT-D) for the 94 elements H-Pu. *J. Chem. Phys.* **2010**, *132*, 154104.

(37) Henkelman, G.; Uberuaga, B. P.; Jonsson, H. A climbing image nudged elastic band method for finding saddle points and minimum energy paths. *J. Chem. Phys.* **2000**, *113*, 9901–9904.

(38) Beyer, A. N.; Richardson, J. O.; Knowles, P. J.; Rommel, J.; Althorpe, S. C. Quantum tunneling rates of gas-phase reactions from on-the-fly instanton calculations. *J. Phys. Chem. Lett.* **2016**, *7*, 4374–4379.

(39) Stamatakis, M.; Vlachos, D. G. A graph-theoretical kinetic Monte Carlo framework for on-lattice chemical kinetics. *J. Chem. Phys.* **2011**, *134*, 214115.

(40) Nielsen, J.; d'Avezac, M.; Hetherington, J.; Stamatakis, M. Parallel kinetic Monte Carlo simulation framework incorporating accurate models of adsorbate lateral interactions. *J. Chem. Phys.* **2013**, *139*, 224706.

(41) Ravipati, S.; D'Avezac, M.; Nielsen, J.; Hetherington, J.; Stamatakis, M. A Caching Scheme To Accelerate Kinetic Monte Carlo Simulations of Catalytic Reactions. *J. Phys. Chem. A* **2020**, *124*, 7140–7154.

(42) Fukui, K. The Path of Chemical-Reactions - the Irc Approach. *Acc. Chem. Res.* **1981**, *14*, 363–368.

(43) Vergés, J. A.; de Andres, P. L. Trapping of electrons near chemisorbed hydrogen on graphene. *Phys. Rev. B* **2010**, *81*, 075423.

(44) Sha, X. W.; Jackson, B. First-principles study of the structural and energetic properties of H atoms on a graphite (0001) surface. *Surf. Sci.* **2002**, *496*, 318–330.

(45) Borodin, V. A.; Vehviläinen, T. T.; Ganchenkova, M. G.; Nieminen, R. M. Hydrogen transport on graphene: Competition of mobility and desorption. *Phys. Rev. B* **2011**, *84*, 075486.

(46) Rooney, J. Eyring transition-state theory and kinetics in catalysis. *J. Mol. Catal. A Chem.* **1995**, *96*, L1–L3.

(47) Jeloaica, L.; Sidis, V. DFT investigation of the adsorption of atomic hydrogen on a cluster-model graphite surface. *Chem. Phys. Lett.* **1999**, *300*, 157–162.

(48) Gillan, M. Quantum Classical Crossover of the Transition Rate in the Damped Double Well. *J. Phys. C: Solid State Phys.* **1987**, *20*, 3621–3641.

(49) Mills, G.; Schenter, G. K.; Makarov, D. E.; Jonsson, H. Generalized path integral based quantum transition state theory. *Chem. Phys. Lett.* **1997**, *278*, 91–96.

(50) Note that the true desorption rate will be even slower than that predicted by instanton theory. This is because instanton theory only models the transition to the physisorbed state and H atoms that reach the physisorbed state via tunnelling do not necessarily have the energy to escape the physisorption well.

(51) Marcus, R.; Coltrin, M. New Tunneling Path for Reactions Such as H+H_2 → H_2+H. *J. Chem. Phys.* **1977**, *67*, 2609–2613.

(52) Chapman, S.; Garrett, B.; Miller, W. Semiclassical Transition-State Theory for Non-separable Systems - Application to Collinear H+H_2 Reaction. *J. Chem. Phys.* **1975**, *63*, 2710–2716.

(53) Skodje, R.; Truhlar, D.; Garrett, B. A General Small-Curvature Approximation for

Transition-State-Theory Transmission Coefficients. *J. Phys. Chem.* **1981**, *85*, 3019–3023.

(54) Greene, S. M.; Shan, X.; Clary, D. C. An investigation of one-versus two-dimensional semiclassical transition state theory for H atom abstraction and exchange reactions. *J. Chem. Phys.* **2016**, *144*, 084113.

(55) Carpenter, B. K. Unearthing the unconventional. *Nat. Chem.* **2010**, *2*, 80–82.

(56) Paris, A. et al. Kinetic Isotope Effect in the Hydrogenation and Deuteration of Graphene. *Adv. Funct. Mater.* **2013**, *23*, 1628–1635.

(57) Limbach, H.-H.; Lopez, J. M.; Kohen, A. Arrhenius curves of hydrogen transfers: tunnel effects, isotope effects and effects of pre-equilibria. *Philos. Trans. R. Soc. B-Biol. Sci.* **2006**, *361*, 1399–1415.

(58) Furuya, K. Isotopic fractionation in interstellar molecules. *Proceedings of the International Astronomical Union* **2017**, *13*, 163–174.

(59) Chen, Y.; Chang, K.-H.; Meng, F.-Y.; Tseng, S.-M.; Chou, P.-T. Broadening the Horizon of the Bell-Evans-Polanyi Principle towards Optically Triggered Structure Planarization. *Angew. Chem. Int. Edit.* **2021**, *60*, 7205–7212.

(60) Krukau, A. V.; Vydrov, O. A.; Izmaylov, A. F.; Scuseria, G. E. Influence of the exchange screening parameter on the performance of screened hybrid functionals. *J. Chem. Phys.* **2006**, *125*, 224106.

(61) Bang, J.; Meng, S.; Sun, Y.-Y.; West, D.; Wang, Z.; Gao, F.; Zhang, S. B. Regulating Energy Transfer of Excited Carriers and the Case for Excitation-Induced Hydrogen Dissociation on Hydrogenated Graphene. *Proc. Natl. Acad. Sci. U.S.A.* **2013**, *110*, 908–911.

TOC Graphic

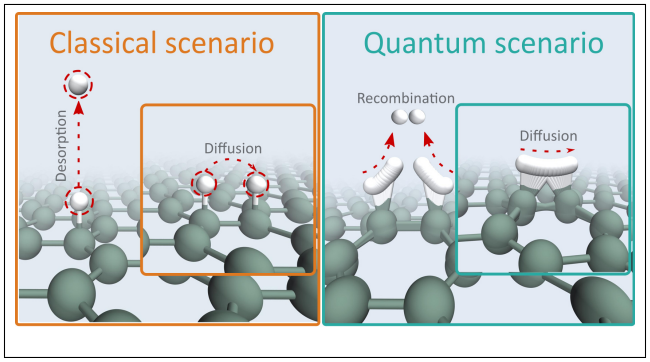
Classical scenario
Desorption
Diffusion
Quantum scenario
Recombination
Diffusion